

WEAK LENSING AS A PROBE OF DARK MATTER¹

L. Van Waerbeke⁽¹⁾, Y. Mellier⁽²⁾

⁽¹⁾ *Observatoire Midi Pyrénées,
14 Av. Edouard Belin,
31400 Toulouse, France*

⁽²⁾ *Institut d'Astrophysique de Paris,
98^{bis} Boulevard Arago,
75014 Paris, France*

Abstract

Weak gravitational lensing of distant galaxies can probe the total projected mass distribution of foreground gravitational structures on all scales and has been used successfully to map the projected mass distribution of rich intermediate redshift clusters. This paper reviews the general concepts of the lensing analysis. We focus on the relation between the observable (shapes and fluxes) and physical (mass, redshift) quantities and discuss some observational issues and recent developments on data analysis which appear promising for a better measurement of the lensing signatures (distortion and magnification) at very large scales.

1 Introduction

The dark matter (DM) component of gravitational structures is extensively studied from the dynamical analysis of the luminous component. Popular examples are the rotation curves of galaxies, motions of galaxies in groups or in clusters, or large scale velocity fields from which the mass and the distribution of the DM can be inferred, provided one assumes a dynamical state (Virial state) and a geometry (sphericity) of the gravitational system. Unfortunately, in most cases these hypotheses are not fulfilled: for example, the Virial hypothesis applied to clusters may be wrong, because clusters may be young gravitational objects. Their mass profile could be alternatively obtained from the X-ray Bremsstrahlung emission of their intra-cluster gas which depends on their total mass distribution and their equilibrium state as well. Again, one has to assume a geometry and a thermodynamical state for the gas of photons and electrons. Despite these difficulties, all these studies provide similar trends, with the mass to light ratio M/L increasing with scale. For a typical galaxy M/L ranges between 10 – 30, but is roughly 10 times larger for a cluster from both Virial and X-ray studies, leading to $\Omega \sim 0.02$ for the former and $\Omega \sim 0.2$ for the later. This means that the mass cannot be concentrated only within the central visible parts of galaxies.

Gravitational lensing provides a direct measurement of the projected mass density without additional hypothesis on the dynamical state or on the geometry of the mass distribution. Provided that we can measure the optical distortion of background objects caused by a foreground

¹To be published in the proceeding of the XXXIst Rencontres de Moriond, Les Arcs, France, January 20-27 1996

mass, it is possible to constrain the projected mass distribution of this deflector. Recent results of the lensing analysis on some clusters are summarized in Table (1).

MASS DISTRIBUTION IN CLUSTERS OF GALAXIES FROM WEAK LENSING

CLUSTER	Z	SCALE	M/L	Z(SOURCE)	REF.
1455+22	0.26	500 Kpc	460		Smail et al. 1994
CI0016+16	0.55	500 Kpc	430		Smail et al. 1994
MS1224	0.33	500 Kpc	800	1.0 -- 2.0	Fahlmann et al. 1994
CI0024+17	0.39	2.5 Mpc	600	0.9 -- 1.2	Bonnet et al. 1994
A1689	0.18	1.0 Mpc	400	1.0 -- 2.0	Tyson & Fischer 1995
A2218	0.18	400 Kpc	440	1.0 -- 2.0	Squires et al. 1995
A2390	0.23	1 Mpc	320	1.0 -- 2.0	Squires et al. 1996
MS1054	0.89	1.9 Mpc	1600 580 350	IF z<1 IF z=1.5 IF z=3	Luppino & Kaiser 1996
A1689	0.18	500 Kpc	>200	1.0 -- 2.0	Broadhurst 1996
A1689	0.18	1 Mpc	400	1.0 -- 2.0	Kaiser 1996
CI0939	0.41	400 Kpc	200	0.6 -- 1.0	Seitz et al. 1996

Table 1: Status of the observations.

These results are larger than the usual Virial or X-Ray analysis by a factor 2 or 3. Whether this discrepancy may be explained or not is not clear yet (Miralda-Escudé & Babul (1995), Navarro et al. (1995)), and we do not discuss this here. We discuss in this paper the general method of the weak lensing analysis leading to these results.

2 The weak lensing analysis

2.1 Basics of gravitational lensing

Because of gravitational lensing, ray-lights are bended and the apparent position $\vec{\theta}_I$ differs from the source position in absence of lensing $\vec{\theta}_S$ by the quantity $\vec{\alpha}$:

$$\vec{\theta}_I = \vec{\theta}_S + \vec{\alpha} \quad (1)$$

where $\vec{\alpha}$ is the gradient of the two-dimensional (projected on the line of sight) gravitational potential ϕ . The gravitational distortion of background objects is described by the Jacobian of the transformation, namely the amplification matrix \mathcal{A} between the source and the image plane (for more details, see Schneider, Ehlers & Falco 1992):

$$\mathcal{A} = \begin{pmatrix} 1 - \kappa - \gamma_1 & -\gamma_2 \\ -\gamma_2 & 1 - \kappa + \gamma_1 \end{pmatrix} \quad (2)$$

where κ is the convergence, γ_1 and γ_2 are the shear components, and are related to the Newtonian gravitational potential ϕ by:

$$\kappa = \frac{1}{2} \nabla^2 \phi = \frac{\Sigma}{\Sigma_{crit}} \quad (3)$$

$$\gamma_1 = \frac{1}{2} (\phi_{,11} - \phi_{,22}) ; \quad \gamma_2 = \phi_{,12} , \quad (4)$$

where Σ is the projected mass density and Σ_{crit} is the critical mass density which depends on the angular diameter distances D_{ij} , ($i, j = (o(bserver), l(ens), s(ource))$) involved in the lens configuration:

$$\Sigma_{crit} = \frac{c^2}{4\pi G} \frac{D_{os}}{D_{ol}D_{ls}} \quad (5)$$

The quantities κ , γ_1 , and γ_2 are not observables. Only the magnification μ and the distortion δ are in principle observable quantities because they are related to the fluxes and the shapes of the objects (Miralda-Escudé 1991, Schneider & Seitz 1995):

$$\mu = \frac{1}{|\mathcal{A}|} = \frac{1}{(1 - \kappa)^2 - \gamma^2} \quad (6)$$

$$\delta_i = \frac{2g_i}{1 + |g|^2} ; \quad g_i = \frac{\gamma_i}{1 - \kappa} \quad (7)$$

Since we are interested in the large scale distribution of the Dark Matter ($> 0.5Mpc$) we only focus the analysis on the weak lensing regime where $(\kappa, \gamma) \ll 1$. The relations between the physical (γ, κ) and observable (δ, μ) quantities become more simple:

$$\mu = 1 + 2\kappa \quad (8)$$

$$\delta_i = 2\gamma_i \quad (9)$$

The projected mass density Σ of the lens is available from the amplification μ using Eq. (8) and Eq. (3), or equivalently from the distortion field by using Eq.(9) and the integration of Eq. (4) (Kaiser, Squires (1993)):

$$\kappa(\vec{\theta}_I) = \frac{-2}{\pi} \int d\vec{\theta} \frac{\chi_i(\vec{\theta} - \vec{\theta}_I) \gamma_i(\vec{\theta}_I)}{(\vec{\theta} - \vec{\theta}_I)^2} + \kappa_0 ; \quad \vec{\chi}(\vec{\theta}) = \left(\frac{\theta_1^2 - \theta_2^2}{\theta^2}, \frac{2\theta_1\theta_2}{\theta^2} \right) \quad (10)$$

κ_0 is the integration constant. In the weak lensing regime, Eqs.(8) and (9) provide two independant methods to map the total projected mass, using the distortion of the background objects and the magnification of the background objects.

2.2 How observable quantities are measured?

The gravitational distortion is not visible on a single galaxy in the weak lensing regime because $\gamma \ll \bar{\epsilon}$, where $\bar{\epsilon}$ is the mean ellipticity of the galaxies. Fortunately a gravitational shear in a given area of the sky distorts all the background galaxies by a same amount, and the distortion can be measured from the mean polarization of these galaxies. The distortion δ_i is computed from the shape of the galaxies in the image plane. Each galaxy is assumed to be elliptical with an ellipticity ϵ and an orientation θ , and is described by a polarization vector $\epsilon e^{2i\theta}$ in a complex formalism. The distortion is given by the sum of the polarization vectors in a given area of the sky. No information is required in the source plane, only the isotropy of the orientation of the galaxies in the source plane is assumed. A detailed description on the optimum detection and measurement of the shape of the galaxies is given in Bonnet & Mellier (1995) and Kaiser et al. (1995). This method has been successfully applied to several clusters (See Table(1)), and to simulations to get the distortion. However, the intrinsic ellipticity of the galaxies is a source of noise, and the contribution of the random orientations of N_g galaxies to the value of the shear γ_i is given by $\bar{\epsilon}/\sqrt{N_g}$. An estimate of the mass using Eq. (10) requires an estimation of Σ_{crit} , which implies the redshift of the sources which is poorly known. Though this is not a critical issue for nearby clusters ($z_l < 0.2$) because $D_{os}/D_{ls} \simeq 1$, it could lead to a large uncertainty of the mass for more distant clusters (See Table (1)).

Unfortunately it is impossible to get a true value for the mass only from the shear map, even if we know the redshift of the sources, because a constant mass plane does not induce any shear on background galaxies. Mathematically, this corresponds to the unknown integration constant κ_0 in Eq.(10). This degeneracy may be broken if one measures the magnification μ which depends on the mass quantity inside the light beam (Eq.(3)). While the shear measurement does not require any information in the source plane, the magnification measurement needs the observation of a reference (unlensed) field to calibrate the magnification. Broadhurst et al. 1995 proposed to compare the number count $N(m, z)$ and/or $N(m)$ in a lensed and an unlensed field to measure μ . Depending on the value of the slope S of the number count in the reference field, we observe a bias (more objects) or an anti-bias (less objects) in the lensed field. The particular value $S = 0.4$ corresponds to the case where the magnification of faint objects is exactly compensated by the dilution of the number count. This method was applied successfully on the cluster A1689 (Broadhurst, 1995), but the signal to noise of the detection remains 5 times lower than with the distortion method for a given number of galaxies. The magnification may also be determined by the changes of the image sizes at fixed surface brightness (Bartelmann & Narayan 1995).

The weakness of these methods is that they require to measure the shape, size and magnitude of very faint objects up to $B=28$, and this is not sure whether the measurement is optimum, and whether systematic effects are avoided. The determination of the shape parameter depends on the threshold level and the convolution mask, and in any cases the information contained in pixels fainter than the threshold level is lost. Furthermore, the measurement of the shape from the second moment matrix is equivalent to the assumption that the objects are elliptical, which is not true. These remarks lead us to propose a new and independent method to analyse the lensing effects, based on the auto-correlation function of the pixels in CCD images, which avoids shape parameter measurements (Van Waerbeke et al. 1996).

3 The Auto-correlation method

3.1 Principle

The CCD image is viewed as a density field rather than an image containing delimited objects. The surface brightness in the image plane in the direction $\vec{\theta}$ is related to the surface brightness in the source plane $I^{(s)}$ by the relation:

$$I(\vec{\theta}) = I^{(s)}(\mathcal{A}\vec{\theta}) \quad (11)$$

and for the auto-correlation function (ACF):

$$\xi(\vec{\theta}) = \xi^{(s)}(\mathcal{A}\vec{\theta}) \quad (12)$$

To understand the meaning of this equation, let us write it in the weak lensing regime:

$$\xi(\vec{\theta}) = \xi^{(s)}(\theta) - \theta \partial_{\theta} \xi^{(s)}(\theta) [1 - \mathcal{A}] \quad (13)$$

$\xi(\vec{\theta})$ is the sum of an isotropic unlensed term $\xi^{(s)}(\theta)$, an isotropic lens term which depends on κ , and an anisotropic term which depends on γ_i .

Let us analyse which gravitational lensing information can be extracted from the shape matrix \mathcal{M} of ξ :

$$\mathcal{M}_{ij} = \frac{\int d^2\theta \xi(\vec{\theta}) \theta_i \theta_j}{\int d^2\theta \xi(\vec{\theta})} \quad (14)$$

The shape matrix in the image plane is simply related to the shape matrix in the source plane $\mathcal{M}^{(s)}$ by $\mathcal{M}_{ij} = \mathcal{A}_{ik}^{-1} \mathcal{A}_{jl}^{-1} \mathcal{M}_{kl}^{(s)}$. If the galaxies are isotropically distributed in the source plane, $\xi^{(s)}$ is isotropic, and in that case $\mathcal{M}_{ij}^{(s)} = M \delta_{ij}$, where δ_{ij} is the identity matrix. Using the expression of the amplification matrix \mathcal{A} we get the general form for \mathcal{M} :

$$\mathcal{M} = \frac{M(a + |g|^2)}{(1 - \kappa)^2(1 - |g|^2)} \begin{pmatrix} 1 + \delta_1 & \delta_2 \\ \delta_2 & 1 - \delta_1 \end{pmatrix} \quad (15)$$

The observable quantities (distortion δ_i and magnification μ) are given in terms of the components of the shape matrix:

$$\delta_1 = \frac{\mathcal{M}_{11} - \mathcal{M}_{22}}{tr\mathcal{M}}; \quad \delta_2 = \frac{2\mathcal{M}_{12}}{tr\mathcal{M}}; \quad \mu = \sqrt{\frac{det\mathcal{M}}{M}} \quad (16)$$

where $tr\mathcal{M}$ is the trace of \mathcal{M} . As for lensed galaxies, we see that the distortion is available from a direct measurement in the image plane while the magnification measurement requires to know the value of M which is related to the light distribution in the source plane, or in an unlensed reference plane. The ACF provides a new and independent way to measure δ_i and μ which does not require shape, size or photometry of individual galaxies. In the following we only describe the measurement of the distortion using this method. The case of the magnification which requires an analysis of the sources galaxies in a reference field, will be developed in a future work.

3.2 The practical method

By definition, the value of the ACF at a pixel position ij is $E_{ij} = \frac{1}{N_{pix}} \sum_{kl} (I_{i+kj+l} - \bar{I})(I_{kl} - \bar{I})$, where I_{kl} is the value of the pixel kl , \bar{I} is the mean value of the image, and N_{pix} the number of terms in the sum. The ACF is computed in a part of the image (a superpixel) where the shear

is assumed to be constant in intensity and direction. Two strategies are possible to compute the ACF. First we can remove all the unwanted objects (stars, bright galaxies, dead CCD lines, cosmetic defaults,...) and compute the ACF from the rest of the image. The main interest of this approach is that it works at the noise level and even ultra faint objects are taken into account. The second approach consists in selecting objects from a given criteria (magnitude, colors, redshift,...), in surrounding them by a large circle, put the rest of the image to zero and compute the ACF of the image containing these circles.

As for the case of individual galaxy we need to compute the shape matrix of the ACF in an annular filter (Bonnet & Mellier, 1995) to avoid the center, where the signal is strongly polluted by the Point Spread Function (PSF), and the external part, which is dominated by the noise. The effects of the PSF and the filter are calibrated by using simulations.

3.3 Sources of errors

The galaxies have not the same flux, size and profile and, by definition of the ACF, are weighted by the square of their flux. Since this could change the statistical properties of the ACF, it is better to work with selected objects by using the second strategy of the ACF method. The idea is to weight each circle which contains an object by a multiplicative term defined as $[\frac{1}{N_{pix}} \sum_{ij} (I_{ij} - \bar{I})^2]^{-1/2}$, where N_{pix} is the number of pixels of the object. The objects are then equally weighted, even when they have very different magnitudes, sizes and profiles.

The intrinsic ellipticity of the galaxies induces a statistical dispersion on the shear estimate of $\sqrt{\bar{\epsilon}/N_g}$, where $\bar{\epsilon}$ is the mean ellipticity of N_g galaxies. Instrumental errors, tracking errors or anisotropic PSF may be removed provided they are measurable on the stellar profiles (Bonnet & Mellier 1995, Kaiser et al. 1995).

The photon noise is a source of error of this method. Indeed, the distortion is computed from one object, the ACF itself. Since the noise polarizes randomly an object, a high noise level makes the measurement of the weak distortion impossible. This lead to the conclusion that a given level of noise corresponds to a distortion threshold γ_0 below which the measured distortion is not reliable. We quantified this threshold from simulations.

4 Conclusion

An optimum analysis of the lensing effects requires the measurement of both the distortion and the magnification to confirm and improve the results quoted in Table (1), and to measure the very weak shear caused by large scale structures. Van Waerkebe et al. (1996) have proposed a new and independent method to measure the gravitational distortion of the background galaxies from the auto-correlation function of the brightness distribution. It does not require any shape, size and centroid determination of individual galaxies, and avoids possible systematics. Moreover the resulting shear is unique and does not depends on the choice of the detection criteria.

The method has been checked on simulated and true data (Q2345 and CL0024). An example of the shear analysis using the ACF on simulated data is shown on Figures 1,2. The shear maps of the real images Q2345 and CL0024 were previously obtained by Bonnet et al. (1993,1994) with the standard method of individual galaxy analysis. Our results are in very good agreement. Moreover, because of the increase of the sensibility with our method, we predict the existence of a new gravitational deflector in the field of Q2345. Further observations will check this point. Because of its simplicity and robustness, this method is well adapted to measure weak shear caused by large scale structure for which a large number of galaxies (~ 100000) is required.

Figure 1: Simulation of a 4 hours exposure at CFHT in the B band on a $3.5'' \times 3.5''$ field. The seeing is $0.7''$ with no tracking errors. Galaxies are lensed by an isothermal sphere ($\sigma = 1000\text{km/s}$), with a core radius of $4''$ located at $200''$ bottom from the field center. The lens redshift is 0.17 and the mean redshift of the sources is 1. The segments show the local orientation of the shear. Their length is proportional to the shear intensity.

Acknowledgements. We thanks P. Schneider, F. Bernardeau and B. Fort for discussions and enthusiastic support. LVW thanks B. Guiderdoni for his invitation and the Moriond's staff for hospitality and financial support.

5 References

- Bartelmann, M., Narayan, R. (1995) ApJ 451, 60.
Bonnet, H., Fort, B., Kneib, J-P., Mellier, Y., Soucail, G. (1993) A&A 280, L7
Bonnet, H., Mellier, Y., Fort, B. (1994) ApJ 427, L83.
Bonnet, H., Mellier, Y. (1995) A&A 303, 331.
Broadhurst, T. (1996) SISSA preprint astro-ph/9511150.
Broadhurst, T., Taylor, A.N., Peacock (1995) ApJ 438, 49.
Fallman, G., Kaiser, N., Squires, G., Woods, D. (1994) ApJ 437. 56.
Kaiser, N. (1996) SISSA preprint astro-ph/9509019.
Kaiser, N., Squires, G. (1993) ApJ 404, 441
Kaiser, N., Squires, G., Broadhurst, T. (1995) ApJ 449, 460.
Luppino, G., Kaiser, N. (1996) SISSA preprint astro-ph/9601194.
Miralda-Escudé, J., Babul, A. (1995) ApJ, 449, 18.
Navarro, J., Frenk, C., White, S. (1995) MNRAS, 275, 720.
Schneider, P., Ehlers, J., Falco, E. E., (1992), *Gravitational Lenses*, Springer.
Schneider, P., Seitz, C. (1995) A&A 294, 411.
Seitz, C., Kneib, J.P., Schneider, P., Seitz, S., (1996) in press.
Smail, I., Ellis, R.S., Fitchett, M. (1994) MNRAS 270, 245.
Squires, G., Kaiser, N., Babul, A., Fahlmann, G., Woods, D., Neumann, D.M., Böhringer, H. (1995) submitted.
Squires, G., Kaiser, N., Fallman, G., Babul, A., Woods, D. (1996) SISSA preprint astro-ph/9602105.
Tyson, J.A., Fisher, P. (1995) ApJL, 349, L1.
Van Waerbeke, L., Mellier, Y., Schneider, P., Fort, B., Mathez, G. (1996) A&A in press.

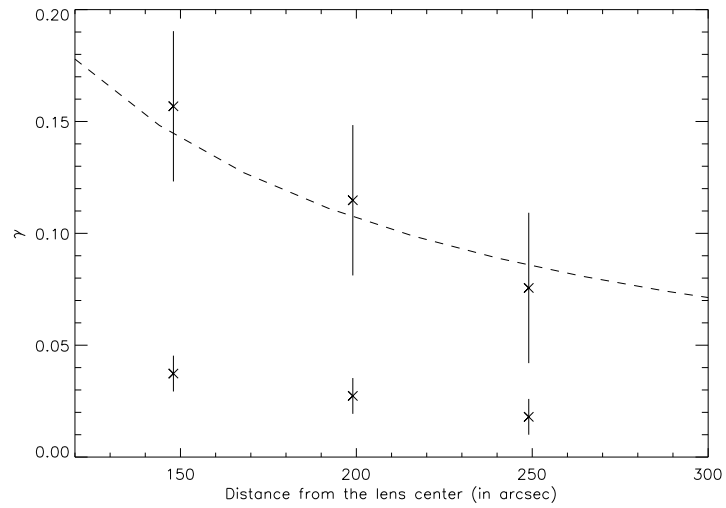


Figure 2: 1-dimensional shear profile from the simulation of Fig.1. At the bottom the uncalibrated measure points are drawn. The theoretically expected shear profile is plotted as the dashed line.

This figure "simul.jpg" is available in "jpg" format from:

<http://arxiv.org/ps/astro-ph/9606100v1>